Nuclear Inst. and Methods in Physics Research, A 958 (2020) 162999

Contents lists available at ScienceDirect

Nuclear Inst. and Methods in Physics Research, A

journal homepage: www.elsevier.com/locate/nima

Development of new large calorimeter prototypes based on $LaBr_3$(Ce) and LYSO crystals coupled to silicon photomultipliers: A direct comparison

A. Papa [a,b,*], P. Schwendimann [b,c]

[a] Dipartimento di Fisica "Enrico Fermi" University of Pisa and INFN, Largo B. Pontecorvo 3, 56127 Pisa, Italy
[b] Paul Scherrer Institute, 5232 Villigen, Switzerland
[c] Swiss Federal Institute of Technology ETH, Rämistrasse 101, 8092 Zurich, Switzerland

ARTICLE INFO

MSC:
00-01
99-00

Keywords:
Calorimeter
High energy gamma detector
Lanthanum Bromide
LYSO
Silicon photomultiplier
Waveform digitiser

ABSTRACT

The challenges for new calorimetry for incoming experiments at the intensity frontier is to provide detectors with ultra-precise time resolution and supreme energy resolution.

Two very promising materials on the market are BrilLanCe (Cerium doped Lanthanum Bromide $LaBr_3$(Ce)) and LYSO (Lutetium Yttrium OxyorthoSilicate, $Lu_{2(1-x)}Y_{2x}SiO_5$(Ce)), supported by recent developments aiming at providing relatively large crystals.

The response of $LaBr_3$(Ce) and LYSO prototypes fired with gammas at an energy of 55 MeV have been studied. Very promising results were obtained.

For the newly available (radius R = 4.45 cm, length L = 20.32 cm) $LaBr_3$(Ce) crystal an energy resolution of $\sigma_E/E \approx 2.36(8)\,\%$ and a timing resolution of $\sigma_t = 35(1)$ ps have been predicted. The energy resolution can be further improved by using larger crystals (either R = 6.35 cm or R = 7.62 cm, L = 20.32 cm) approaching respectively a $\sigma_E/E = 1.20(3)\,\%$ or a $\sigma_E/E = 0.91(1)\,\%$.

Due to the shorter radiation length X_0 and smaller Molière radius (R_M) a LYSO crystal of the available size (radius R = 3.5 cm, L = 16 cm) performs better in terms of energy deposit compared to the currently available larger crystal made of LaBr3(Ce). An energy resolution of $\sigma_E/E = 1.48(4)\,\%$ can be obtained, further improved by using bigger crystals (R = 6.5 cm, L = 25 cm) to $\sigma_E/E = 0.74(1)\,\%$. A timing resolution less performing than the $LaBr_3$(Ce) but better than any nowadays available calorimeter working at this energy can be achieved and is expected to be $\sigma_t = 49(1)$ ps.

Such results put these materials coupled to silicon photomultipliers at the detector forefront for future high energy calorimetry at the intensity frontier.

1. Introduction: The $LaBr_3$(Ce) and LYSO main scintillation properties

The challenges for new calorimetry for incoming experiments at the intensity frontier is to provide detectors with ultra-precise time resolution and supreme energy resolution [1–6].

Two very promising materials on the market are BrilLanCe (Cerium doped Lanthanum Bromide $LaBr_3$(Ce)) and LYSO (Lutetium Yttrium OxyorthoSilicate, $Lu_{2(1-x)}Y_{2x}SiO_5$(Ce)), supported by recent developments aiming at providing relatively large crystals [7–10].

Cerium doped Lanthanum Bromide stands out due to its ultra-high light yield (1.65 x NaI(Tl)) and by a more than an order of magnitude faster decay time compared to NaI(Tl). With these properties together with its high density, $LaBr_3$(Ce) is the ideal medium for calorimetry limited only by the currently available crystal size on the market [11].

Due to recent developments, larger crystals up to a radius R = 4.45 cm and a length L = 20.3 cm can be produced commercially. A calorimeter build from such a large crystal is an eligible candidate for the detection of gammas at energies from few tens up one hundred MeV. This corresponds to the interesting energy range of current charged Lepton Flavour Violating (cLFV) experiments. Thus $LaBr_3$(Ce) may be a suitable candidate for future experiments in this sector.

LYSO on the other hand exhibits a very high density, comparable to BGO and thus features short radiation length X_0 and Molière radius R_M. Despite the fact that the light yield is only roughly 70% of NaI and the decay time roughly three times longer compared to $LaBr_3$(Ce), its density makes LYSO an attractive candidate as well — especially considering that the available crystal size is one of the limiting factors.

Table 1 summarises the main scintillation properties compared to the widely used scintillation media. For a quick comparison a Figure of Merit (F.o.M.) is defined as the square root of the ratio of the scintillation decay time τ and the product of the light output LY and the density ρ.

* Corresponding author at: Dipartimento di Fisica "Enrico Fermi" University of Pisa and INFN, Largo B. Pontecorvo 3, 56127 Pisa, Italy.
E-mail addresses: angela.papa@unipi.it, angela.papa@psi.ch (A. Papa), patrick.schwendimann@psi.ch (P. Schwendimann).

https://doi.org/10.1016/j.nima.2019.162999
Received 1 April 2019; Received in revised form 11 October 2019; Accepted 17 October 2019
Available online 19 October 2019

Table 1
Main scintillation properties for widely used scintillator media. A F.o.M. is given as defined in the text.

Scintillator	Density ρ (g/cm^3)	Light yield LY (ph/keV)	Decay time τ (ns)	F.o.M. $\sqrt{\tau/(\rho \cdot LY)}$
$LaBr_3$(Ce)	5.08	63	16	0.22
LYSO	7.1	27	41	0.46
YAP	5.35	22	26	0.47
LXe	2.89	40	45	0.62
NaI(Tl)	3.67	38	250	1.34
BGO	7.13	9	300	2.16

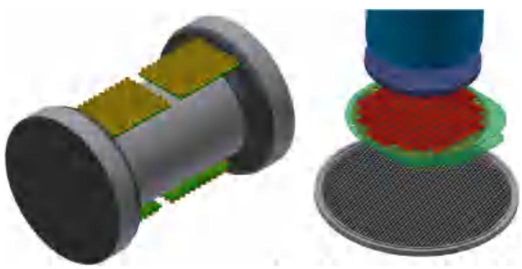

Fig. 1. The first large crystal assembly for high energy gamma $\mathcal{O}(50)$ MeV detection with a MPPC double readout scheme. The assembly is the same for both kinds of crystals, $LaBr_3$(Ce) and LYSO.

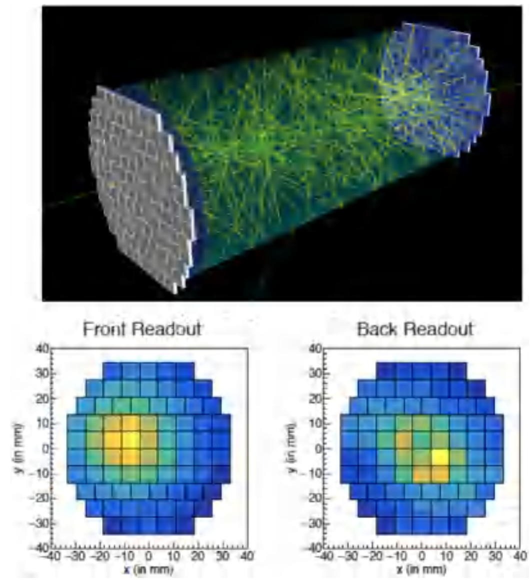

Fig. 2. Sketch of the scintillation light distribution associated to a 55 MeV gamma event impinging on (R = 3.5 cm, L = 16 cm) LYSO crystal coupled to Hamamatsu S13360-6025PE (top) and the typical collected charge distribution on the front and back face (bottom).

2. A new generation of segmented calorimeters: Large crystals coupled to silicon photomultipliers

These already exciting features can be improved even further by coupling the crystals to state of the art Multi-Pixel Photon Counters (MPPCs), commonly called Silicon photomultipliers (SiPMs). The result is a detector with a high photosensor granularity, high rate sustainability, maximal photosensor coverage area, optimal geometrical acceptance and that is insensitive to magnetic fields. Due to their small thickness of a few mm even the radiation impinging area can be covered with minimal impact on gammas passing through it. Independent of the chosen crystal a lot of light will be generated. To keep saturation effects at a minimum, the smallest available pixel size for the MPPCs is considered. In addition, the granularity due to the MPPCs allows some geometrical reconstruction of the event.

Two different MPPC candidates by different manufacturers are investigated (Hamamatsu S13360-6025PE and sensL MicroFJ-60035TSV) [12,13].

The Monte Carlo simulations are based on the Geant4 libraries with dedicated code that includes the MPPC's response and the whole electronic chain up to the DAQ, based on waveform digitiser with a sampling frequency up to 5 GSample/s [14–17]. The reconstructed algorithms are based on waveform analysis. The simulations are supported by measurements done with available $LaBr_3$(Ce) crystals with sizes of (R = 3.81 cm, L = 7.62 cm) and (R= 1.27 cm, L = 10.16 cm) coupled to either photomultiplier tubes or MPPCs and the characterisation of the MPPC response.

3. $LaBr_3$(Ce) And LYSO large prototype calorimeters: Expected performances

For the first time the response of these two prototypes fired with gammas with an energy of 55 MeV have been studied. Unless stated otherwise the photons hit the centre of the crystal. The assembly of the detectors is shown in Fig. 1.

The first new feature of these prototypes is the double readout scheme. The MPPCs are mounted also on the front/entrance face, through which the radiation impinges into the detector. This feature improves the photon detection efficiency by more than a factor of two w.r.t. the single backside readout due to the energy deposit near the entrance face. This is a typical characteristic of dense materials such as $LaBr_3$(Ce) and LYSO. Fig. 2 sketches the scintillation light distribution associated to a 55 MeV gamma event impinging on a (R = 3.5 cm, L = 16 cm) LYSO crystal coupled to Hamamatsu S13360-6025PE (top) and the typical collected charge distribution on the front and back face (bottom). Fig. 3 shows quantitatively the double readout improvements on the energy resolution for a given crystal and MPPCs assembly. The histograms representing the number of detected photons are fitted by a tailed gaussian function given by:

$$f(x|N,\mu,\sigma_1,\sigma_2,\sigma_3) = \begin{cases} N \cdot \exp\left(-\frac{(\mathrm{x}-\mu)^2}{2\sigma_1^2}\right) \\ \text{if } \mathrm{x} \le \mu; \\ N \cdot \exp\left(-\frac{(\mathrm{x}-\mu)^2}{2(\sigma_1+\sigma_2(\mathrm{x}-\mu)+\sigma_3(\mathrm{x}-\mu)^2)^2}\right) \\ \text{if } \mathrm{x} > \mu. \end{cases} \quad (1)$$

Figs. 4–6 summarise the main results about the energy, timing and position resolution for different detector assemblies. Here the time t_0 is that at which the gamma enters inside the detector. The used algorithm is the weighted average among the timing calculated with the constant fraction (threshold = 15%) of the most intense amplitude and its neighbours. In formula:

$$t_0 = \frac{(n-1)t_f + (n+1)t_b - \frac{L}{c}n(n+1)}{2n} \quad (2)$$

where $t_{f,b}$ are the reconstructed time on the front and back faces respectively, n and L the refractive index and the length of the crystal respectively and c the speed of light. For the (R = 4.45 cm, L = 20.3 cm) $LaBr_3$(Ce) crystal an energy resolution of $\sigma_{\mathrm{E/E}} \approx 2.3(1)\%$ and a timing resolution of $\sigma_{\mathrm{t}} \approx 35(1)$ ps have been predicted. The energy resolution can be further improved by using larger crystals (either R = 6.35 cm or R = 7.6 cm, L = 20.32 cm) approaching respectively a $\sigma_{\mathrm{E/E}} \approx 1.20(3)\%$ and a $\sigma_{\mathrm{E/E}} \approx 0.96(1)\%$.

Due to the shorter radiation length and smaller Molière radius a LYSO crystal of the available size (R = 3.5 cm, L = 16 cm) performs better in terms of energy deposit compared to the currently available larger crystal made of $LaBr_3$(Ce). An energy resolution of $\sigma_{\mathrm{E/E}} \approx 1.48(4)\%$ can be obtained, and that can be further improved using bigger crystals (R = 6.5 cm, L = 25 cm), $\sigma_{\mathrm{E/E}} \approx 0.74(1)\%$. A timing

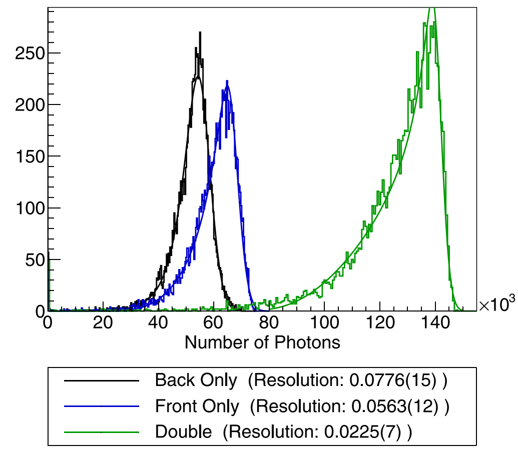

Fig. 3. Different readout schemes based on Hamamatsu S13360-6025PE MPPC for a (R = 4.45 cm and L = 20.32 cm) LaBr3(Ce) crystal. The additional matter on the front side due to the MPPC and support structures does not have any observable impact on the energy deposit. The front-only readout scheme detects more photons than the back-only readout scheme. The combination of the two yields the most promising results.

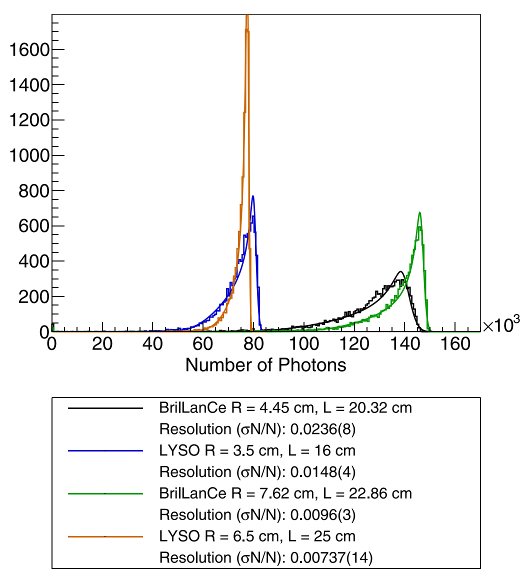

Fig. 4. Energy resolutions and number of detected photons for $LaBr_3$(Ce) and LYSO crystals of different sizes.

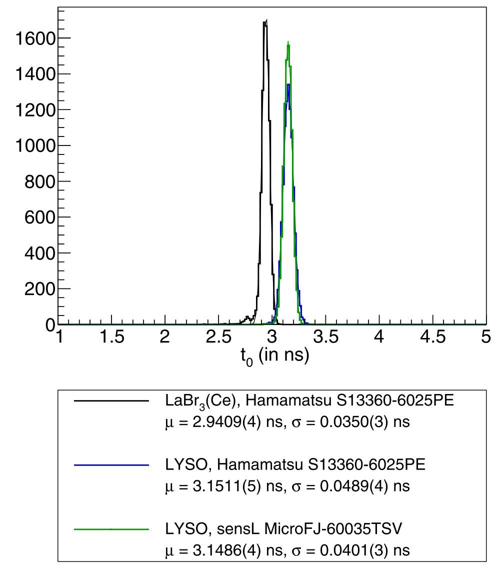

Fig. 5. Timing resolutions for the available (R = 4.45 cm, L = 20.32 cm) $LaBr_3$(Ce) and (R = 3.5 cm, L = 16 cm) LYSO crystals. Here the $LaBr_3$(Ce) is coupled to the Hamamatsu S13360-6025PE. For the LYSO both MPPC options (Hamamatsu S13360-6025PE and sensL MicroFJ-60035TSV) are displayed.

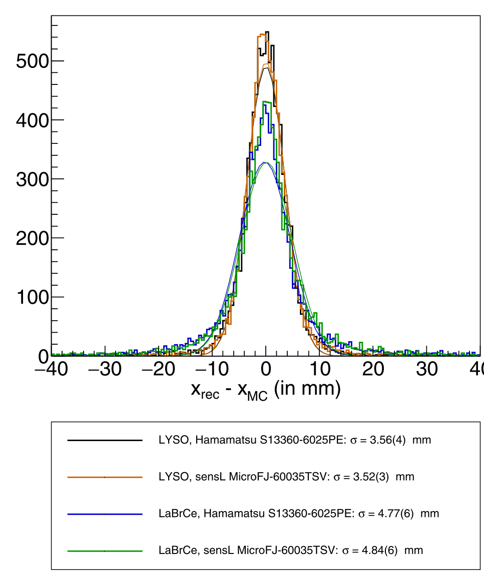

Fig. 6. X variable resolutions for the available (R = 4.45 cm, L = 20.32 cm) $LaBr_3$(Ce) and (R = 3.5 cm, L = 16 cm) LYSO crystals. Both MPPC options (Hamamatsu S13360-6025PE and sensL MicroFJ-60035TSV) are displayed.

resolution less performing than the $LaBr_3$(Ce) one but better than any available nowadays calorimeter working at this energy can be obtained and is expected to be $\sigma_t \approx 49(1)$ ps. By coupling the LYSO to the sensL SiPMs (MicroFJ-60035TSV) instead of the Hamamatsu ones (S13360-6025PE), the timing resolution can be improved to 40 ps. This is due to the better coverage and PDE that results in increased photon statistics.

The three-dimensional event reconstruction performances are very similar for both detector configurations presented in Fig. 6. The x and y variables are symmetrical and only the x variable is shown. A $\sigma_x \approx \sigma_y$ in the range of 3.5 – 5 mm is quoted depending on the detector configuration. The reconstructed x is calculated combining linearly the reconstructed x on both the front (x_f) and back (x_b) faces using the relationship:

$$x_{\rm rec} = a\overline{x}_f + b\overline{x}_b + c. \qquad (3)$$

The parameters a, b and c are estimated by an individual fit method comparing $x_{\rm rec}$ to $x_{\rm MC}$ for each crystal geometry in use. A σ_z in the range of 5.2 – 6 mm is quoted, depending of the detector configuration.

The reconstructed z is obtained by combining both the timing and collected charge on both front and back faces using the formula:

$$z_{\rm rec} = at_f + bt_b + b + c \ln N_f + d \ln N_b + e \qquad (4)$$

where $t_{f,b}$ are the reconstructed times using the constant fraction method and $N_{f,b}$ the collected photons on the front and back faces respectively and the five parameters a, b, c, d and e are estimated based on an individual fitting algorithm.

Until now we have considered point-like gamma sources impinging the front face of the different detector configurations. In practice, unless the source is strongly collimated, we have to deal with extended sources. In our case we expect to have a uniform 4π gamma source at a distance of 60 cm from the detector. In this case, following a simplified view, two types of events can be considered: the inner and the border events. The later spoils the detector performances due to leakage effects. The highly segmented photosensor coverage can be used as a powerful analysis tool. Geometrical cuts can be applied for an optimal trade-off between kinematical variable resolutions and event selection efficiency. This is particularly important in view of a segmented/multi-element scalable big calorimeter. Several methods can be considered from the straightforward reconstructed radius cut up to others like the skewness cut based on the expected Monte Carlo simulated asymmetrical charge distribution. The bigger the crystal the higher the selection efficiency. Actually for crystals with radii greater than 7.5 cm for the $LaBr_3$(Ce) and 6.5 cm for the LYSO the extended source performance approaches the point-like ones with an event selection efficiency greater than 80%.

These new calorimeters with such estimated performances are currently at the detector frontiers.

4. Conclusions

The challenges for new calorimetry for incoming experiments at intensity frontier is to provide detectors with ultra-precise time resolution and supreme energy resolution.

New detectors have been considered here for the first time based on either large $LaBr_3$(Ce) or LYSO crystals coupled to MPPCs showing very promising results for high energy gamma $\mathcal{O}(50)$ MeV calorimetry. Independent of the specific detector assembly, simultaneous energy, timing and position resolutions below 1 MeV, 50 ps and 6 mm appear to be feasible. Such results put this new calorimetry at the detector forefront for particle physics research at beam intensity frontiers.

Acknowledgements

The authors thank the Paul Scherrer Institute as host laboratory. This work was supported in part by the SNF, Switzerland 200020_172706 and by MIUR, Italy Montalcini D.M. 2014 n. 975.

References

[1] J. Adam, et al., (MEG collaboration), Eur. Phys. J. C 73 (2013) 2365.
[2] J. Adam, et al., (MEG collaboration), Phys. Rev. Lett. 110 (2013) 201801.
[3] A.M. Baldini, et al., (MEG collaboration), Eur. Phys. J. C 76 (2016) 434.
[4] A.M. Baldini, et al., (MEGII collaboration), Eur. Phys. J. C 78 (2018) 380.
[5] G. Cavoto, et al., Eur. Phys. J. C 78 (2018) 37.
[6] F. Berg, et al., Phys. Rev. Acc. Beams 19 (2016) 024701.
[7] M. Ciemala, et al., Nucl. Instrum. Methods A 608 (2009) 76.
[8] L. Galli, et al., Nucl. Instrum. Methods A 718 (2013) 48.
[9] A. Papa, et al., Nuclear Phys. B 248–250 (2014) 115.
[10] A. Papa, P. Schwendimann, Nucl. Instrum. Methods A 936 (2019) 130.
[11] https://www.crystals.saint-gobain.com.
[12] http://www.hamamatsu.com/us/en/index.html.
[13] https://sensl.com.
[14] S. Agostinelli, et al., Nucl. Instrum. Methods A 506 (2003) 250.
[15] A. Papa, et al., JINST 9 (2014) C05066.
[16] S. Ritt, et al., Nucl. Instrum. Methods A 623 (2010) 486.
[17] A. Stoykov, et al., Nucl. Instrum. Methods A 695 (2012) 202.